

Performance comparison of optimization algorithms in LQR controller design for a nonlinear system

Ümit ÖNEN^{1,*}, Abdullah ÇAKAN², İlhan İLHAN¹

¹Department of Mechatronics Engineering, Faculty of Engineering and Architecture, Necmettin Erbakan University, Konya, Turkey

²Department of Mechanical Engineering, Faculty of Engineering and Natural Sciences, Konya Technical University, Konya, Turkey

Received: 06.08.2018

Accepted/Published Online: 03.03.2019

Final Version: 15.05.2019

Abstract: The development and improvement of control techniques has attracted many researchers for many years. Especially in the controller design of complex and nonlinear systems, various methods have been proposed to determine the ideal control parameters. One of the most common and effective of these methods is determining the controller parameters with optimization algorithms. In this study, LQR controller design was implemented for position control of the double inverted pendulum system on a cart. First of all, the equations of motion of the inverted pendulum system were obtained by using Lagrange formulation. These equations were linearized by Taylor series expansion around the equilibrium position to obtain the state-space model of the system. The LQR controller parameters required to control the inverted pendulum system were determined by using a trial and error method. The determined parameters were optimized by using five different configurations of three different optimization algorithms (GA, PSO, and ABC). The LQR controller parameters obtained as a result of the optimization study with five different configurations of each algorithm were applied to the system and the obtained results were compared with each other. In addition, the configurations that yielded the best control results for each algorithm were compared with each other and the control results were evaluated in terms of response speed and response smoothness.

Key words: Artificial bee colony algorithm, genetic algorithm, inverted pendulum, LQR control, optimization, particle swarm optimization

1. Introduction

Researchers have been studying the development and improvement of control techniques for many years. Inverted pendulums (IPs), especially the cart versions, are among the most commonly used systems for design and comparison of the control techniques due to their nonlinear and unstable structures. IPs are a good example of underactuated systems where the number of variables to be controlled is greater than the number of control inputs. These specifications make pendulum systems ideal to investigate the performance of control techniques. Furthermore, IPs and their extensions including springs, dampers, and actuators have been used as a representative model of the human body or biped robots for investigation of the kinematics, kinetics, and balance properties [1–5].

On the other hand, IP systems have been widely used to examine the performances of various control techniques. Linear control methods such as proportional integral derivative (PID) [6, 7] and linear quadratic

*Correspondence: uonen@erbakan.edu.tr

regulator (LQR) [7, 8] have been used in the control of IPs. PID control is one of the simplest and efficient control methods for various control problems. It presents a generic and effectual solution in the case that the control parameters are tuned appropriately. The linear quadratic regulator (LQR) is an optimal and state-space feedback controller widely used in various fields of industry. It uses performance index and state matrices to calculate the optimal control inputs. The performance of the LQR mainly depends on the determination of weight matrices (Q and R). The determination of the control parameters and weigh matrices for both PID and LQR control is usually performed by trial and error and depends on the designer's experience. Use of trial and error method to determine control parameters not only takes much time but also does not guarantee finding the best solution possible. On the other hand, the use of a linearized system model may cause instability and poor closed-loop system behavior. Nonlinear control techniques such as feedback linearization [9] and back stepping [10], output feedback stabilization [11], delayed feedback [12], H infinity [13], and sliding mode [6, 14, 15] techniques have been developed for the control of IP systems. Although the nonlinear control techniques have shown desirable performance in tracking and stabilization problems of nonlinear systems, they are the most difficult and complicated control techniques in implementation. Intelligent control techniques such as fuzzy logic [16, 17] and neural network [18] controllers have been used in the control of IP systems. Although intelligent control techniques offer advantages such as simple construction and low computational requirements, they cannot guarantee stability. Furthermore, the NN-based controller requires a large dataset obtained from experiments for training and the FLC requires a complex rule base for higher order systems. Model predictive control (MPC) has been used in the control of IPs [19, 20]. MPC uses the system model for predicting the future behavior of the controlled variables. The performance of the controller directly depends on the system model, but the difficulty in obtaining an accurate model for complex systems is the major disadvantage of MPC control.

As can be seen, almost all control techniques have several advantages and disadvantages when used alone. Various hybrid control methods such as PID + sliding mode control [21], fuzzy logic + sliding mode control [22, 23], and neural network + fuzzy logic control [24] that combine one or more different control techniques have been developed for eliminating these disadvantages. On the other hand, one of the biggest problems in controller design, especially for nonlinear systems, is the determination of ideal controller parameters. Heuristic or trial-error methods are often used in determination of control parameters but these techniques do not guarantee finding the best solution possible. Besides, they are quite time-consuming and challenging. In recent years, optimization algorithms have begun to be used in determination of controller parameters for linear or nonlinear systems. Optimization algorithms are single-solution or population-based metaheuristic algorithms and generally perform good approximation for the best solution for all kind of problems. The genetic algorithm [25–28], particle swarm optimization [25, 27, 29–33], artificial bee colony algorithm [34–38], ant colony optimization [39, 40], firefly algorithm [41, 42], bat algorithm [43–46], gray wolf optimization [47–49], antlion optimization [50], cuckoo search optimization [51, 52], etc. have been used to optimize parameters of different control algorithms designed to control various linear and nonlinear systems.

In this study, the use of optimization algorithms to determine the parameters of an LQR controller designed to control a nonlinear system has been investigated. A double IP system on a cart, which is quite difficult to control due to the nonlinear and underactuated system characteristics, has been chosen as the control plant. The genetic algorithm (GA), particle swarm optimization (PSO), and artificial bee colony (ABC), which are well-known high-performance algorithms, have been used to optimize the parameters of the LQR controller. The performances of the optimization algorithms have been evaluated and compared through simulations. The

paper is organized as follows. In Section 2, the mathematical model of the DIP system is derived by Lagrange formulation. The derived equations are linearized around an equilibrium position with Taylor series expansion and the state-space model of the system is obtained. In Section 3, design of the LQR controller for the position control of the DIP system is carried out. In Section 4, optimization of the parameters of the designed LQR controller by GA, PSO, and ABC algorithms is presented. In Section 5, the simulation results of the optimized LQR controllers and the comparison of the performances of the optimization algorithms are presented. Finally, the conclusions of the study are explained in Section 6.

2. Mathematical model of double inverted pendulum on a cart

The model of the double IP on a cart is shown in Figure 1. The system consists of a cart and two pendulums connected to each other with rotary joints. m_0 , m_1 , and m_2 denote the mass of the cart, lower pendulum, and upper pendulum, respectively. L_1 and L_2 denote the length of the lower and upper pendulums, respectively. The pendulums can swing freely in the $x - y$ plane, whereas the car can move right and left along the x -axis. The force F denotes the external force applied to the car along the x -axis. The aim of the control is to move the cart to a desired position as soon as possible while ensuring pendulums remain in the vertical direction. This system is a good example of underactuated systems because control of three degrees of freedom (DOF) is carried out only by the force F applied to the car. The Lagrangian of the system can be defined as;

$$L = T - V, \tag{1}$$

where L is the Lagrangian, T is the total kinetic energy, and V is the total potential energy of the system. Dynamic equations of the system can be derived by the Lagrange equations given in Eq. (2):

$$\frac{d}{dt} \left(\frac{\partial L}{\partial \dot{q}} \right) - \frac{\partial L}{\partial q} = Q_i. \tag{2}$$

In this equation, q_i is the generalized coordinates and Q_i is the generalized forces.

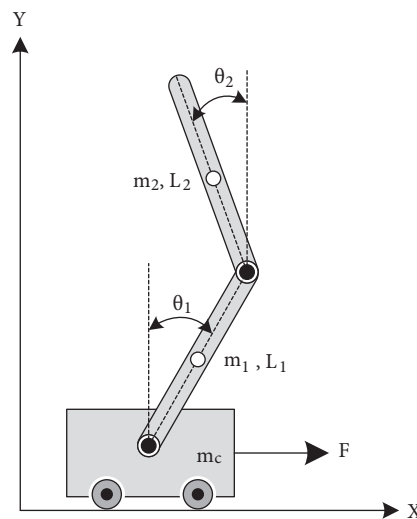


Figure 1. Double inverted pendulum system on a cart.

For this problem, generalized coordinates can be defined as follows:

$$q(t)^T = [x(t) \quad \theta_1(t) \quad \theta_2(t)], \tag{3}$$

where $x(t)$ is the position of the cart in the horizontal axis, and $\theta_1(t)$ and $\theta_2(t)$ are the angle of the first and second pendulum relative to the vertical direction. The generalized force of the system is F . If the total kinetic energy and the total potential energy are written in Eq. (1), the Lagrangian of the system can be obtained as below:

$$\begin{aligned} &= \frac{1}{2} \left\{ I_1 \dot{\theta}_1^2 + I_2 \dot{\theta}_2^2 + m_0 \dot{x}^2 + m_1 \left(\dot{x}^2 + \frac{1}{4} L_1^2 \dot{\theta}_1^2 + \dot{x} L_1 \cos \theta_1 \dot{\theta}_1 \right) \right\} \\ &\quad + \frac{1}{2} m_2 \left\{ \left(\dot{x}^2 + L_1^2 \dot{\theta}_1^2 + \frac{1}{4} L_2^2 \dot{\theta}_2^2 + 2 \dot{x} L_1 \cos \theta_1 \dot{\theta}_1 + \dot{x} L_2 \cos \theta_2 \dot{\theta}_2 + L_1 L_2 \cos \theta_1 \dot{\theta}_1 \sin \theta_2 \dot{\theta}_2 \right) \right\} \\ &\quad - \left\{ \frac{1}{2} m_1 g L_1 \cos \theta_1 + m_2 g L_1 \cos \theta_1 + \frac{1}{2} m_2 g L_2 \cos \theta_2 \right\}. \tag{4} \end{aligned}$$

The dynamic equations of the system can be obtained as below by substituting Eq. (4) into Eq. (2).

$$\begin{aligned} a \ddot{x} + b \cos \theta_1 \ddot{\theta}_1 + c \cos \theta_2 \ddot{\theta}_2 - b \sin \theta_1 \dot{\theta}_1^2 - c \sin \theta_2 \dot{\theta}_2^2 &= F, \\ b \cos \theta_1 \ddot{x} + d \ddot{\theta}_1 + e \cos(\theta_2 - \theta_1) \ddot{\theta}_2 + e \sin(\theta_1 - \theta_2) \dot{\theta}_2^2 - b g \sin \theta_1 &= 0, \\ c \cos \theta_2 \ddot{x} + e \cos(\theta_2 - \theta_1) \ddot{\theta}_1 + f \ddot{\theta}_2 + e \dot{\theta}_1^2 \sin(\theta_2 - \theta_1) - c g \sin \theta_2 &= 0. \end{aligned} \tag{5}$$

In these equations, $a = (m_0 + m_1 + m_2)$, $b = (\frac{1}{2} m_1 L_1 + m_2 L_1)$, $c = (\frac{1}{2} m_2 L_2)$, $d = (I_1 + \frac{1}{4} m_1 L_1^2 + m_2 L_1^2)$, $e = (\frac{1}{2} m_2 L_1 L_2)$, $f = (I_2 + m_2 L_2^2)$.

The equilibrium point of the system can be defined as $[x \quad \theta_1 \quad \theta_2 \quad \dot{x} \quad \dot{\theta}_1 \quad \dot{\theta}_2] = [0 \quad 0 \quad 0 \quad 0 \quad 0 \quad 0]$. Dynamic equations can be linearized around the equilibrium point by Taylor series expansion assuming that the system makes small oscillations. The state-space model of the system can be expressed as below:

$$\begin{aligned} \dot{x} &= Ax + Bu, \\ y &= Cx + Du, \end{aligned} \tag{6}$$

where x denotes the states and y denotes the outputs of the system. The states and the outputs of the system can be defined as:

$$\begin{aligned} x^T &= [x_1 \quad x_2 \quad x_3 \quad x_4 \quad x_5 \quad x_6] = [x \quad \theta_1 \quad \theta_2 \quad \dot{x} \quad \dot{\theta}_1 \quad \dot{\theta}_2], \\ y^T &= [x_1 \quad x_2 \quad x_3]. \end{aligned} \tag{7}$$

The system parameters used in calculations are given in Table 1. The state and the output matrix of the system can be calculated as follows by using Eq. (5), Eq. (6), and the parameters given in Table 1.

$$A = \begin{bmatrix} 0 & 1 & 0 & 0 & 0 & 0 \\ 0 & 0 & 6.192 & 0 & -0.7120 & 0 \\ 0 & 0 & 0 & 1 & 0 & 1 \\ 0 & 0 & 81.206 & 0 & -71.173 & 0 \\ 0 & 0 & 0 & 0 & 0 & 1 \\ 0 & 0 & -88.35 & 0 & 124.788 & 0 \end{bmatrix} \quad B = \begin{bmatrix} 0 \\ 0.05933 \\ 0 \\ 3.0112 \\ 0 \\ -3.2763 \end{bmatrix} \quad C = \begin{bmatrix} 1 & 0 & 0 & 0 & 0 & 0 \\ 0 & 0 & 1 & 0 & 0 & 0 \\ 0 & 0 & 0 & 0 & 1 & 0 \\ 0 & 1 & 0 & 0 & 0 & 0 \\ 0 & 0 & 0 & 1 & 0 & 0 \\ 0 & 0 & 0 & 0 & 0 & 1 \end{bmatrix} \quad D = \begin{bmatrix} 0 \\ 0 \\ 0 \\ 0 \\ 0 \\ 0 \end{bmatrix} \tag{8}$$

Table 1. Parameters of the double inverted pendulum system.

Parameter	Definition	Value
m_0	Mass of cart	1.5 kg
m_1	Mass of the first pendulum	0.5 kg
m_2	Mass of the second pendulum	0.75 kg
L_1	Length of the first pendulum	0.5 m
L_2	Length of the second pendulum	0.75 m
I_1	Moments of inertia of the first pendulum around the joint	0.0416 kgm ²
I_2	Moments of inertia of the second pendulum around the joint	0.14 kgm ²

3. Design of the LQR controller

The LQR is an optimal state-space feedback controller for linear systems that is widely used in various fields of industry. The LQR uses state variables and performance index J to calculate an optimal control input. Considering the linear state-space equation given in Eq. (6), the aim of the LQR is to determine the optimal control law $u = K.(ref - x)$, which minimizes the performance index J given by

$$J = \int_0^{\infty} (q_{ref}(t) - q(t))^T Q (q_{ref}(t) - q(t)) + u(t)^T R u(t) dt. \tag{9}$$

In the LQR controller design, the system input is calculated by using Q and R diagonal matrices to reduce the performance index J . The symmetric positive semidefinite matrix Q and symmetric positive definite matrix R can be defined as below:

$$Q = \begin{bmatrix} q_1 & 0 & 0 \\ 0 & \ddots & 0 \\ 0 & 0 & q_n \end{bmatrix}, \quad R = \begin{bmatrix} r_1 & 0 & 0 \\ 0 & \ddots & 0 \\ 0 & 0 & r_m \end{bmatrix}. \tag{10}$$

Basically, matrix Q adjusts the distribution of the control effect over the states while matrix R adjusts the aggressiveness of the control. The LQR gain vector K is expressed as:

$$K = R^{-1} B^T P. \tag{11}$$

In this equation, P is a positive definite symmetric constant matrix obtained from the solution of the algebraic Ricatti equation given in Eq. (12):

$$A = A^T P + Q - P B R^{-1} B^T P = 0. \tag{12}$$

In the determination of LQR parameters, the trial and error method has been widely used. Generally, this method presents satisfactory results after troublesome and time-consuming trials, but it cannot be known whether the obtained results are the best or not. On the other hand, many optimization methods such as the GA and PSO have been used to determine LQR parameters [13–18]. Although the optimization algorithms increase the computational load, they guarantee almost the best results in the specified parameter range.

The optimized LQR control scheme of the double inverted pendulum is given in Figure 2. Inputs of the controller are the position and velocity errors of the card, the first pendulum and the second pendulum, expressed as $e_c = X_r - X$, $\dot{e}_c = \dot{X}_r - \dot{X}$, $e_{1p} = \theta_{1r} - \theta_1$, $\dot{e}_{1p} = \dot{\theta}_{1r} - \dot{\theta}_1$, $e_{12} = \theta_{2r} - \theta_2$, $\dot{e}_{2p} = \dot{\theta}_{2r} - \dot{\theta}_2$,

respectively. Output of the controller is the force applied to the cart (F). The LQR controller calculates the control force F according to gain vector K . Optimization algorithms use the objective function and input–output pairs of the system to optimize Q and R matrices and determine the best gain vector K of the LQR controller.

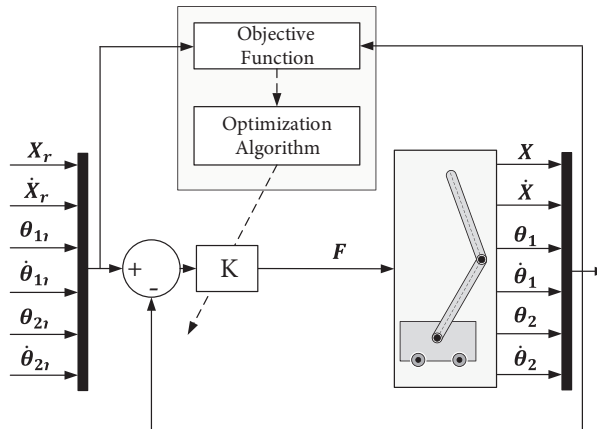


Figure 2. Optimized LQR control scheme of double inverted pendulum system on a cart.

4. Optimization of the LQR controller

4.1. Genetic algorithm

The GA is a search technique used to find approximate solutions to optimization problems. It was proposed by John Holland in 1975, inspired by genetic operations such as mutation, crossover, and selection. The flowchart of the GA is given in Figure 3. It starts with a population consisting of randomly generated individuals (chromosomes) represented by 0s and 1s. The solutions of the previous population are used to produce a new population. In each generation (iteration), the fitness of each chromosome is evaluated according to the objective function of the optimization problem and the natural selection process is realized according to these fitness values. After selection, the crossover and mutation processes are applied to the population. The crossover process creates a new generation with selected chromosomes while the mutation process changes a small fraction of the bits in the chromosomes. The new generation of candidate solutions is then used in the next generation of the algorithm. It is expected that the newly created population is better than the current population since the more fit chromosomes are selected. This process is repeated until the appropriate solution or maximum iteration number is reached. The population size and crossover and mutation rates given as inputs are the critical parameters affecting the performance of algorithm. The GA may not achieve a perfect solution since it does not produce a lot of different states to choose the best, unlike the broad search algorithms, but it is one of the best algorithm taking time constraints into consideration.

4.2. Particle swarm optimization

The PSO algorithm is a population-based heuristic search technique used to find solutions to optimization problems. It was developed by Kennedy and Eberhart, inspired by the social behavior of bird and fish swarms. The flowchart of PSO is given in Figure 4.

The PSO algorithm begins by creating an initial population (swarm) consisting of randomly generated particles within an initialization region. Random position and velocity assigned particles search the optimum

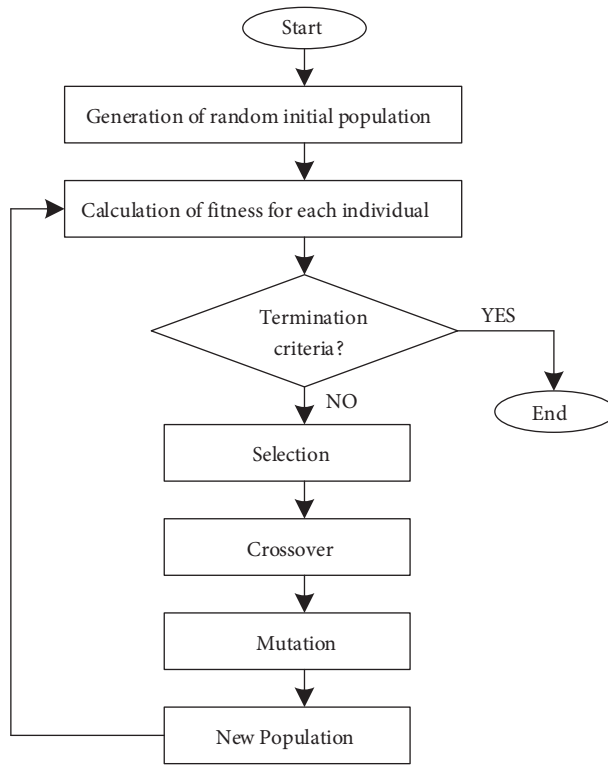


Figure 3. Flowchart of the genetic algorithm.

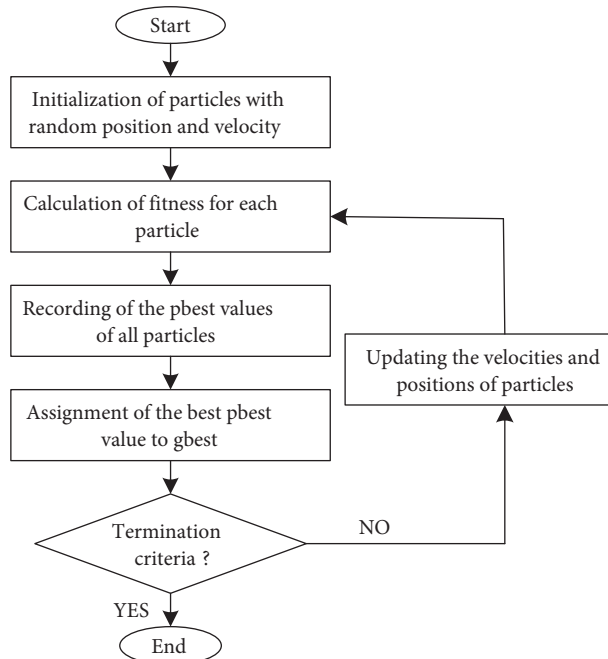


Figure 4. Flowchart of the PSO algorithm.

solution by navigating in the problem space. The position of each particle corresponds to a candidate solution of the optimization problem represented by objective function f . The fitness of each particle is calculated

according to the objective function f and the best position ($pbest$) ever visited by that particle is determined. After the determination of the $pbest$ value of each particle in the population, the best position ever visited by any particle ($gbest$) is determined. The velocities and the positions of the particles are calculated by Eqs. (14) and (15), respectively:

$$v_{ij}^{k+1} = w \cdot v_{ij}^k + c_1 \cdot r_1 \cdot (pbest_{ij}^k - x_{ij}^k) + c_2 \cdot r_2 \cdot (gbest_{ij}^k - x_{ij}^k), \quad (13)$$

$$x_{ij}^{k+1} = x_{ij}^k + v_{ij}^{k+1}. \quad (14)$$

In these equations, c_1 and c_2 are the learning factors and w is the inertia weight. The learning factor leads the movement of a particle according to its own experience and the experience of the other particles in the swarm. The inertia weight adjusts the extent of the search area. A small inertia weight enables the local search while a large inertia weight allows the global search. After the update, the fitness of each particle in the new population is recalculated. This process is repeated until the appropriate solution or maximum iteration number is reached.

4.3. Artificial bee colony algorithm

The ABC algorithm is an intelligent search technique used to find solutions to optimization problems. It was proposed by Karaboğa, inspired by the behavior of honey bee swarms that find a food source and share the knowledge of this food source with others [35, 36]. The ABC algorithm divides the artificial bees in a bee colony into three groups as employed bees, onlooker bees, and scout bees. The employed bees search the food sources in the field and share the information of food sources with other bees. Each employed bee is responsible for only one food source. The onlooker bees wait in the hive and find a food source according to information provided by the employed bees. An employed bee turns into a scout bee after draining the food source and starts to search for new food sources around the hive. The position of a food source means a candidate solution for the corresponding problem. The value of the objective function represented by the nectar amount determines the quality of solution. The flowchart of the ABC algorithm is given in Figure 5.

The algorithm starts with random distribution of employed bees in the search field and production of the initial solutions. For $i = 1, 2, \dots, SN$ (SN is the number of source), each source is a D -dimensional vector. The position of the i th food source in the search space is represented by $X_i = (X_{i1} \ X_{i2} \ \dots \ X_{iD})^T$. Each employed bee searches and produces a modified food source position by the following equation:

$$x'_{ij} = x_{ij} + r_{ij}(x_{ij} - x_{kj}), \quad (15)$$

where $j \in 1, 2, \dots, D$ and $k \in 1, 2, \dots, SN$ are randomly chosen indices and $k \neq i$. The parameter r_{ij} is also a real random number in the domain $[-1, 1]$. After receiving the food source information the onlooker bee goes to the food source region at X_i based on probability P_i defined by the following equation:

$$P_i = \frac{fit_i}{\sum_{n=1}^{SN} fit_n}. \quad (16)$$

Fitness value fit_i is calculated by using the following equation:

$$fit_i = \begin{cases} \frac{1}{1+f(X_i)} & f(X_i) \geq 0 \\ 1 + |f(X_i)| & f(X_i) < 0, \end{cases} \quad (17)$$

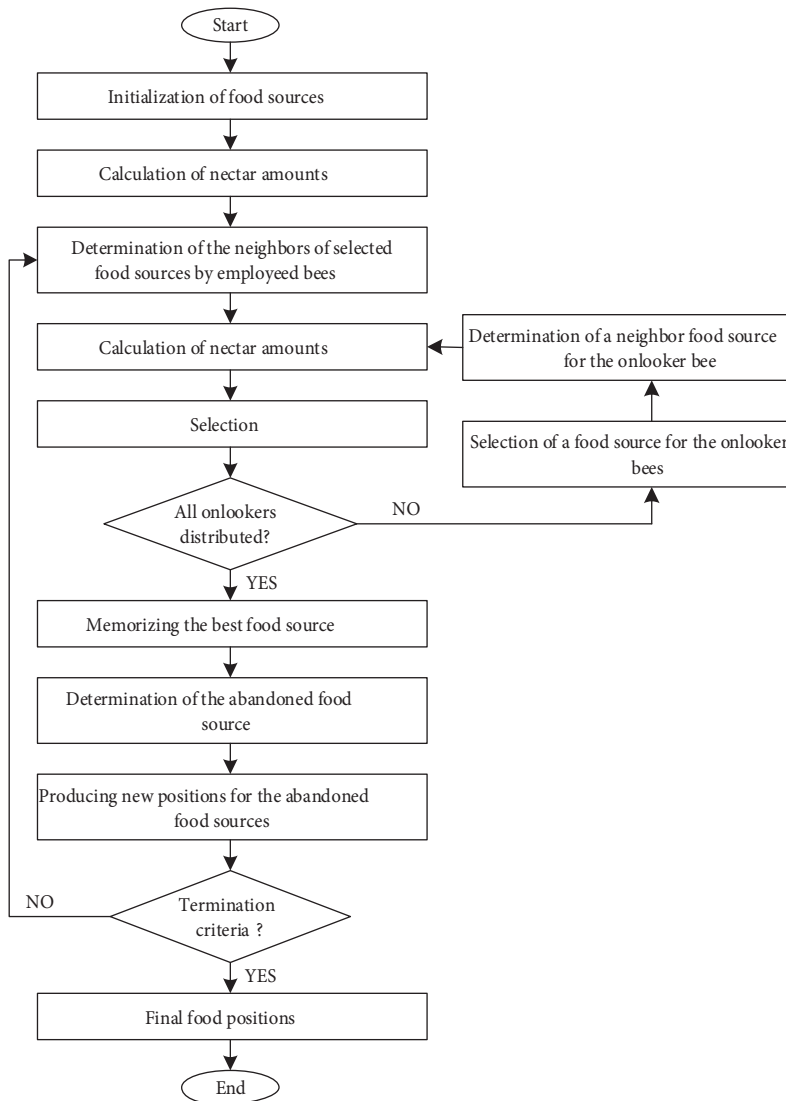


Figure 5. Flowchart of the ABC algorithm.

where $f(X_i)$ is the objective function of source X_i to be minimized. If the new fitness value is better than the previous fitness values, than the bee moves to this new food source. The source information is shared with the onlooker bees after the process is completed by all employed bees and each onlooker bee selects a food source by the probability given above. Each bee searches a better food source until the appropriate solution or maximum iteration number is reached.

5. Results and discussion

The difficulties in determination of LQR weighting matrices by trial and error method were explained in Section 3. In addition, it is almost impossible to find the best controller parameters by trial and error method. In this study, an LQR controller is designed by trial and error method and then three different optimization algorithms (GA, PSO, and ABC) are used to optimize Q and R matrices and increase the control performance of the designed LQR controller. The aim of the control is to move the cart to the desired position as soon as possible

while ensuring that the pendulums remain in a vertical direction. For this aim, the objective function is selected as in Eq. (18) to minimize the parameters of peak time (t_p), rise time (t_r), settling time (t_s), steady state error (x_{sse}), and maximum peak (x_{max}), which are obtained from the time response of the system:

$$\begin{aligned}
 J_e = & (x_{t_p} + x_{t_r} + x_{t_s} + x_{max} + x_{e_{ss}}) \\
 & +(\theta_{1_{norm}} + \theta_{1_{t_s}} + \theta_{1_{t_p}} + \theta_{1_{max}} + \theta_{1_{e_{ss}}}) \\
 & +(\theta_{2_{norm}} + \theta_{2_{t_s}} + \theta_{2_{t_p}} + \theta_{2_{max}} + \theta_{2_{e_{ss}}}).
 \end{aligned}
 \tag{18}$$

In order to obtain the best control performance, the gain matrix of the LQR is optimized by the GA, PSO, and ABC algorithms for five different parameter configurations. Obtained results and gain matrices of the LQR controller for five different configurations of the GA, PSO, and ABC algorithms are given in Table 2, Table 3, and Table 4, respectively. In these tables GN denotes the number of generations, PN denotes the number of populations, IN denotes the number of iterations, and SN denotes the number of sources. Elite count and crossover rate is selected as $PN/5$ and 0.7, respectively, for the GA. Learning factors c_1 and c_2 and inertia weight w are selected as 2, 2, and 0.7, respectively, for PSO. Employed bee number and trial number are selected as 1 and 10, respectively, for the ABC algorithm. These are the best values determined by trial and error.

Table 2. Genetic algorithm optimization results for different configurations.

GA		1st Configuration		2nd Configuration		3rd Configuration		4th Configuration		5th Configuration	
		GN	PN	GN	PN	GN	PN	GN	PN	GN	PN
		10	10	20	10	20	20	50	20	50	50
Q	q1	536.5944		633.9251		362.6393		477.1877		369.562	
	q2	5.7138		2.6905		4.2827		4.2853		0.9444	
	q3	709.8085		897.6025		937.3992		907.1489		948.2754	
	q4	3.1626		9.9907		6.8276		7.1498		2.9315	
	q5	916.4022		733.2397		615.0272		383.9576		873.2419	
	q6	9.2384		4.1905		8.4089		9.4682		4.0263	
R	r1	0.2002		0.2290		0.0974		0.1372		0.1197	
Gain Matrix (K)		[51.7730 -257.3899 -592.8469 55.0546 -96.6268 -95.6808]		[52.6091 -261.9908 -600.2279 55.7859 -98.2218 -96.9284]		[61.0284 -337.2715 -752.5058 67.6568 -123.8328 -122.1510]		[58.9784 -306.9173 -685.2538 63.6184 -113.1199 -111.5963]		[55.5582 -296.9583 -661.4884 60.6483 -109.2807 -106.7161]	
Min. Error (S)		2861.4448		2854.7185		2846.0569		2845.5725		2839.5729	
Elapsed Time (s)		42.9582		82.0706		162.8280		319.3512		806.3919	

Control results for the LQR controller optimized by each configuration of the GA, PSO, and ABC are given in Figures 6a–6c, respectively. Each configuration of the three algorithms can successfully optimize the gain matrix of the LQR controller. However, since the selected objective function includes many parameters obtained from the time response of the system, it is necessary to decide the control target more clearly in order to determine which algorithm is more successful. The results obtained for the controller optimized with the GA are very similar to each other as seen from Figure 6a. While the fastest control response is obtained for the 1st configuration, the smoothest control response is obtained for the 3rd configuration. The results obtained for the controller optimized with the PSO algorithm are more sensitive to the configuration changes, as seen in Figure 6b. For the PSO algorithm, while the fastest control response is obtained for the 1st configuration, the smoothest control response is obtained for the 4th configuration. The algorithm that is the most sensitive to configuration changes is ABC, as seen in Figure 6c. For the ABC algorithm, while the fastest control response is obtained for the 5th configuration, the smoothest control response is obtained for the 4th configuration.

Table 3. Particle swarm optimization results for different configurations.

PSO		1st Configuration		2nd Configuration		3rd Configuration		4th Configuration		5th Configuration	
		IN	PN	IN	PN	IN	PN	IN	PN	IN	PN
		10	10	20	10	20	20	50	20	50	50
Q	q ₁	421.963		173.046		165.9793		145.461		120.3213	
	q ₂	4.715		0.01		2.4404		0.01		0.01	
	q ₃	999.969		1000		1000		1000		936.4859	
	q ₄	5.416		6.596		10		3.063		0.01	
	q ₅	559.269		777.944		1000		999.608		211.0802	
	q ₆	6.253		4.703		1.601		10		10	
R	r ₁	0.126		0.024		0.02025		0.01		0.01	
Gain Matrix (K)		[57.6473 -308.7550 -684.7843 63.1202 -113.3882 -111.1594]		[1.0e+03 [0.0836 -0.5456 -1.1753 0.0988 -0.1950 -0.1902]		[1.0e+03 [0.0905 -0.6125 -1.3208 0.1092 -0.2192 -0.2128]		[1.0e+03 [0.1206 -0.8299 -1.7552 0.1452 -0.2918 -0.2852]		[1.0e+03 [0.1097 -0.7548 -1.5475 0.1323 -0.2613 -0.2553]	
Min. Error (S)		2847.268		2827.150		2826.1599		2823.2926		2822.2097	
Elapsed Time (s)		29.072		60.942		124.199		298.773		755.550	

Table 4. Artificial bee algorithm optimization results for different configurations.

ABC		1st Configuration		2nd Configuration		3rd Configuration		4th Configuration		5th Configuration	
		IN	SN	IN	SN	IN	SN	IN	SN	IN	SN
		10	10	20	10	20	20	50	20	50	50
Q	q ₁	265.3566		85.8085		77.3344		115.0397		112.5518	
	q ₂	6.7337		0.07034		2.7705		0.01		0.01	
	q ₃	642.3138		545.9471		994.8526		796.6027		0.01	
	q ₄	2.7289		3.2128		2.7532		3.7631		6.5282	
	q ₅	433.3621		444.2493		803.3359		990.4651		1000	
	q ₆	7.8179		3.4252		1.6468		5.2735		4.0406	
R	r ₁	0.0694		0.01		0.01		0.01		0.01	
Gain Matrix (K)		[61.8282 -340.7263 -752.1528 68.7999 -124.4864 -122.5426]		[1.0e+03 [0.0926 -0.6227 -1.3371 0.1108 -0.2215 -0.2166]		[1.0e+03 [0.0879 -0.7104 -1.4842 0.1162 -0.2484 -0.2376]		[1.0e+03 [0.1073 -0.7414 -1.5852 0.1296 -0.2626 -0.2554]		[1.0e+03 [0.1061 -0.5478 -1.2993 0.1115 -0.2063 -0.2075]	
Min. Error (S)		2849.6543		2828.2825		2825.1782		2819.9062		2816.4768	
Elapsed Time (s)		71.269		126.1446		243.8559		625.1855		1563.3592	

The configurations that give the fastest and smoothest control results of each algorithm are compared with each other in 7a and 7b, respectively. As can be seen in Figure 7a, optimization algorithms give very similar results in terms of the response speed. Although the GA gives slightly better results in terms of response speed, the settling times of the cart, the first pendulum, and the second pendulum are about 2 s, 3 s, and 2 s, respectively, for all algorithms. The comparison of the optimization algorithms in terms of response smoothness is given in Figure 7b. The smoothest control results are obtained from the ABC while the GA has the worst performance. The maximum peak of the first and the second pendulum is obtained as -0.075 rad and -0.04 rad for the ABC and -0.125 rad and -0.06 rad for the GA. On the other hand, settling time of the cart is 4.5 s for the ABC and 3 s for the GA; settling time of the first pendulum is 4 s for the ABC and 3 s for the GA; and settling time of the second pendulum is 3 s for the ABC and 2 s for the GA.

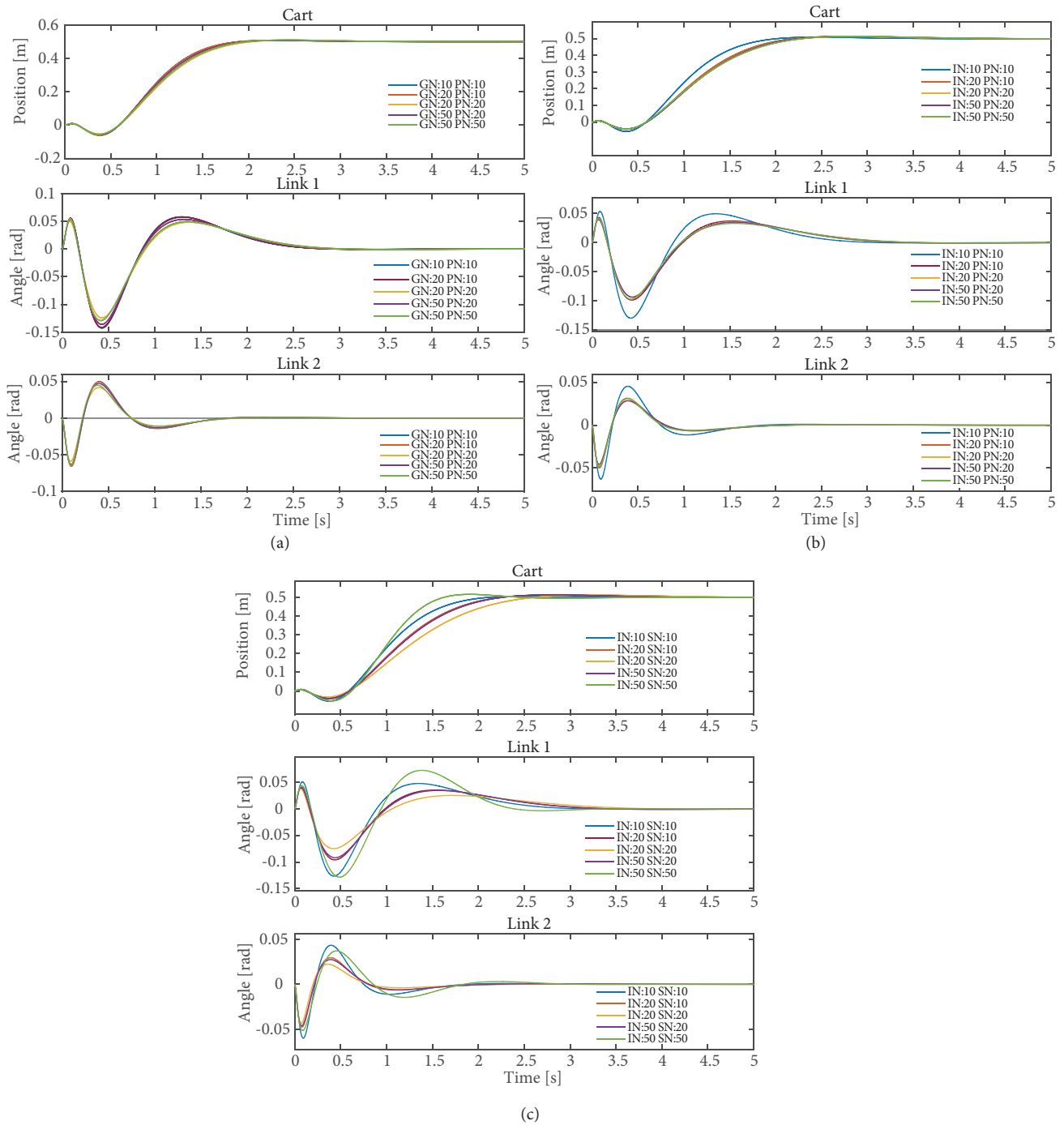


Figure 6. Results of the LQR controller optimized with different configurations of algorithms: ?? GA, ?? PSO, and ?? ABC.

6. Conclusion

In this study, the performances of three different optimization algorithms (GA, PSO, and ABC) in the determination of LQR controller parameters are investigated. The objective function for the optimization is selected so as to account for all important parameters of the control response such as peak time, rise time, settling

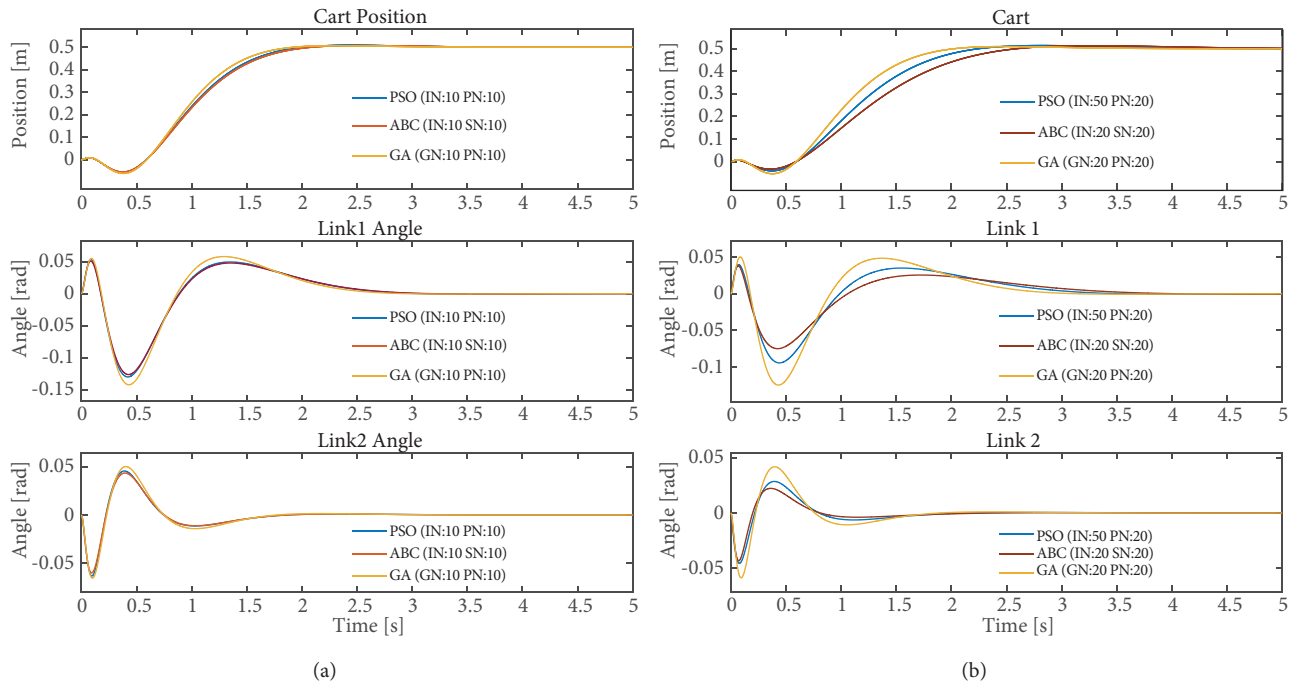


Figure 7. Comparison of the optimization algorithms in terms of control response: ?? response speed, ?? response smoothness.

time, steady state error, and maximum peak. In order to obtain the best optimization result, five different configurations of each algorithm have been tested and the configurations that yield the best control results for each algorithm are compared with each other. All three algorithms have successfully optimized the LQR controller parameters and presented very close control results. The control results were evaluated in terms of response speed and response smoothness. According to the results, the controller optimized by the GA gave the fastest control response, while the smoothest response was provided by the controller optimized by the ABC algorithm.

References

- [1] Hong H, Kim S, Kim C, Lee S, Park S. Spring-like gait mechanics observed during walking in both young and older adults. *Journal of Biomechanics* 2013; 46 (1): 77-82.
- [2] Koolen T, De Boer T, Rebula J, Goswami A, Pratt J. Capturability-based analysis and control of legged locomotion, Part 1: Theory and application to three simple gait models. *International Journal of Robotics Research* 2012; 31 (9): 1094-1113.
- [3] McGrath M, Howard D, Baker R. The strengths and weaknesses of inverted pendulum models of human walking. *Gait & Posture* 2015; 41 (2): 389-394.
- [4] Pratt J, Koolen T, De Boer T, Rebula J, Cotton S et al. Capturability-based analysis and control of legged locomotion, Part 2: Application to M2V2, a lower-body humanoid. *International Journal of Robotics Research* 2012; 31 (10): 1117-1133.
- [5] Suzuki Y, Nomura T, Casadio M, Morasso P. Intermittent control with ankle, hip, and mixed strategies during quiet standing: a theoretical proposal based on a double inverted pendulum model. *Journal of Theoretical Biology* 2012; 310: 55-79.

- [6] Nasir A, Ismail R, Ahmad M. Performance comparison between sliding mode control (SMC) and PD-PID controllers for a nonlinear inverted pendulum system. *World Academy of Science, Engineering, and Technology* 2010; 71: 400-405.
- [7] Prasad LB, Tyagi B, Gupta HO. Optimal control of nonlinear inverted pendulum dynamical system with disturbance input using PID controller & LQR control system. In: 2011 IEEE International Conference on Control System, Computing and Engineering; 25–27 November 2011; Penang, Malaysia. pp. 540-545.
- [8] Zhang J, Zhang W. LQR self-adjusting based control for the planar double inverted pendulum. *Physics Procedia* 2012; 24: 1669-1676.
- [9] Ibanez CA, Frias OG, Castanon MS. Lyapunov-based controller for the inverted pendulum cart system. *Nonlinear Dynamics* 2005; 40 (4): 367-374.
- [10] Jabbar A, Malik FM, Sheikh SA. Nonlinear stabilizing control of a rotary double inverted pendulum: a modified backstepping approach. *Transactions of the Institute of Measurement and Control* 2017; 39 (11): 1721-1734.
- [11] Lee J, Mukherjee R, Khalil HK. Output feedback stabilization of inverted pendulum on a cart in the presence of uncertainties. *Automatica* 2015; 54: 146-157.
- [12] Landry M, Campbell SA, Morris K, Aguilar CO. Dynamics of an inverted pendulum with delayed feedback control. *SIAM Journal on Applied Dynamical Systems* 2005; 4 (2): 333-351.
- [13] Ashok Kumar M, Kanthalakshmi S. H_∞ tracking control for an inverted pendulum. *Journal of Vibration and Control* 2018; 24: 3515–3524. doi: 10.1177/1077546317750977
- [14] Wai RJ, Chang LJ. Adaptive stabilizing and tracking control for a nonlinear inverted-pendulum system via sliding-mode technique. *IEEE Transactions on Industrial Electronics* 2006; 53 (2): 674-692.
- [15] Wang JJ. Stabilization and tracking control of X-Z inverted pendulum with sliding-mode control. *ISA Transactions* 2012; 51 (6): 763-770.
- [16] Tao CW, Taur JS, Wang C, Chen U. Fuzzy hierarchical swing-up and sliding position controller for the inverted pendulum–cart system. *Fuzzy Sets and Systems* 2008; 159 (20): 2763-2784.
- [17] Roose AI, Yahya S, Al-Rizzo H. Fuzzy-logic control of an inverted pendulum on a cart. *Computers & Electrical Engineering* 2017; 61: 31-47.
- [18] Jung S, Cho HT, Hsia TC. Neural network control for position tracking of a two-axis inverted pendulum system: experimental studies. *IEEE Transactions on Neural Networks* 2007; 18 (4): 1042-1048.
- [19] Messikh L, Guechi EH, Benloucif M. Critically damped stabilization of inverted-pendulum systems using continuous-time cascade linear model predictive control. *Journal of the Franklin Institute* 2017; 354 (16): 7241-7265.
- [20] Jung S, Wen JT. Nonlinear model predictive control for the swing-up of a rotary inverted pendulum. *Journal of Dynamic Systems, Measurement, and Control* 2004; 126 (3): 666-673.
- [21] Mahmoodabadi M, Taherkhorsandi M, Talebipour M, Castillo-Villar K. Adaptive robust PID control subject to supervisory decoupled sliding mode control based upon genetic algorithm optimization. *Transactions of the Institute of Measurement and Control* 2015; 37 (4): 505-514.
- [22] Lin CM, Mon YJ. Decoupling control by hierarchical fuzzy sliding-mode controller. *IEEE Transactions on Control Systems Technology* 2005; 13 (4): 593-598.
- [23] Soltanpour MR, Khooban MH, Khalghani MR. An optimal and intelligent control strategy for a class of nonlinear systems: adaptive fuzzy sliding mode. *Journal of Vibration and Control* 2016; 22 (1): 159-175.
- [24] Saifizul A, Zainon Z, Osman NA, Azlan C, Ibrahim UU. Intelligent control for self-erecting inverted pendulum via adaptive neuro-fuzzy inference system. *American Journal of Applied Sciences* 2006; 3 (4): 1795-1802.
- [25] Oh SK, Jang HJ, Pedrycz W. A comparative experimental study of type-1/type-2 fuzzy cascade controller based on genetic algorithms and particle swarm optimization. *Expert Systems with Applications* 2011; 38 (9): 11217-11229.

- [26] Jesus IS, Barbosa RS. Genetic optimization of fuzzy fractional PD+ I controllers. *ISA Transactions* 2015; 57: 220-230.
- [27] Sabzi HZ, Humberson D, Abudu S, King JP. Optimization of adaptive fuzzy logic controller using novel combined evolutionary algorithms, and its application in Diez Lagos flood controlling system, Southern New Mexico. *Expert Systems with Applications* 2016; 43: 154-164.
- [28] Martínez R, Castillo O, Aguilar LT. Optimization of interval type-2 fuzzy logic controllers for a perturbed autonomous wheeled mobile robot using genetic algorithms. *Information Sciences* 2009; 179 (13): 2158-2174.
- [29] Zamani M, Karimi-Ghartemani M, Sadati N, Parniani M. Design of a fractional order PID controller for an AVR using particle swarm optimization. *Control Engineering Practice* 2009; 17 (12): 1380-1387.
- [30] Liu CH, Hsu YY. Design of a self-tuning PI controller for a STATCOM using particle swarm optimization. *IEEE Transactions on Industrial Electronics* 2010; 57 (2): 702-715.
- [31] Saleem A, Taha B, Tutunji T, Al-Qaisia A. Identification and cascade control of servo-pneumatic system using particle swarm optimization. *Simulation Modelling Practice and Theory* 2015; 52: 164-179.
- [32] Dhillon SS, Lather J, Marwaha S. Multi objective load frequency control using hybrid bacterial foraging and particle swarm optimized PI controller. *International Journal of Electrical Power & Energy Systems* 2016; 79: 196-209.
- [33] Ufnalski B, Kaszewski A, Grzesiak LM. Particle swarm optimization of the multioscillatory LQR for a three-phase four-wire voltage-source inverter with an *LC* output filter. *IEEE Transactions on Industrial Electronics* 2015; 62 (1): 484-493.
- [34] Ata B, Coban R. Artificial bee colony algorithm based linear quadratic optimal controller design for a nonlinear inverted pendulum. *International Journal of Intelligent Systems and Applications in Engineering* 2015; 3 (1): 1-6.
- [35] Karaboga D, Basturk B. A powerful and efficient algorithm for numerical function optimization: artificial bee colony (ABC) algorithm. *Journal of Global Optimization* 2007; 39 (3): 459-471.
- [36] Karaboga D, Basturk B. On the performance of artificial bee colony (ABC) algorithm. *Applied Soft Computing* 2008; 8 (1): 687-697.
- [37] Karaboga D, Gorkemli B, Ozturk C, Karaboga N. A comprehensive survey: artificial bee colony (ABC) algorithm and applications. *Artificial Intelligence Review* 2014; 42 (1): 21-57.
- [38] Rajasekhar A, Abraham A, Pant M. A hybrid differential artificial bee colony algorithm based tuning of fractional order controller for permanent magnet synchronous motor drive. *International Journal of Machine Learning and Cybernetics* 2014; 5 (3): 327-337.
- [39] Bououden S, Chadli M, Karimi HR. An ant colony optimization-based fuzzy predictive control approach for nonlinear processes. *Information Sciences* 2015; 299: 143-158.
- [40] Castillo O, Neyoy H, Soria J, Melin P, Valdez F. A new approach for dynamic fuzzy logic parameter tuning in ant colony optimization and its application in fuzzy control of a mobile robot. *Applied Soft Computing* 2015; 28: 150-159.
- [41] Debbarma S, Saikia LC, Sinha N. Automatic generation control using two degree of freedom fractional order PID controller. *International Journal of Electrical Power & Energy Systems* 2014; 58: 120-129.
- [42] Pradhan PC, Sahu RK, Panda S. Firefly algorithm optimized fuzzy PID controller for AGC of multi-area multi-source power systems with UPFC and SMES. *Engineering Science and Technology International Journal* 2016; 19 (1): 338-354.
- [43] Dash P, Saikia LC, Sinha N. Automatic generation control of multi area thermal system using bat algorithm optimized PD-PID cascade controller. *International Journal of Electrical Power & Energy Systems* 2015; 68: 364-372.
- [44] Premkumar K, Manikandan B. Bat algorithm optimized fuzzy PD based speed controller for brushless direct current motor. *Engineering Science and Technology International Journal* 2016; 19 (2): 818-840.

- [45] Abd-Elazim S, Ali E. Load frequency controller design via BAT algorithm for nonlinear interconnected power system. *International Journal of Electrical Power & Energy Systems* 2016; 77: 166-177.
- [46] Rahmani M, Ghanbari A, Ettefagh MM. Robust adaptive control of a bio-inspired robot manipulator using bat algorithm. *Expert Systems with Applications* 2016; 56: 164-176.
- [47] Sharma Y, Saikia LC. Automatic generation control of a multi-area ST–Thermal power system using Grey Wolf Optimizer algorithm based classical controllers. *International Journal of Electrical Power & Energy Systems* 2015; 73: 853-862.
- [48] Lal DK, Barisal A, Tripathy M. Grey wolf optimizer algorithm based fuzzy PID controller for AGC of multi-area power system with TCPS. *Procedia Computer Science* 2016; 92: 99-105.
- [49] Guha D, Roy PK, Banerjee S. Load frequency control of interconnected power system using grey wolf optimization. *Swarm and Evolutionary Computation* 2016; 27: 97-115.
- [50] Raju M, Saikia LC, Sinha N. Automatic generation control of a multi-area system using ant lion optimizer algorithm based PID plus second order derivative controller. *International Journal of Electrical Power & Energy Systems* 2016; 80: 52-63.
- [51] Jin Q, Qi L, Jiang B, Wang Q. Novel improved cuckoo search for PID controller design. *Transactions of the Institute of Measurement and Control* 2015; 37 (6): 721-731.
- [52] Berrazouane S, Mohammedi K. Parameter optimization via cuckoo optimization algorithm of fuzzy controller for energy management of a hybrid power system. *Energy Conversion and Management* 2014; 78: 652-660.